Performance Evaluation for Absolute Time Synchronization in Wireless Time-Sensitive Service

Yong Sun Kim
ETRI
Daejeon, Korea
doori@etri.re.kr

Kapseok Chang
ETRI
Daejeon, Korea
kschang@etri.re.kr

Young-Jo Ko
ETRI
Daejeon, Korea
koyj@etri.re.kr

***Abstract*—**As mobile devices such as robots and automobiles are diversified, demand for wireless time-sensitive services is increasing rapidly. In this paper, we propose a new frame structure to meet the absolute time synchronization (ATS) requirement for wireless time-sensitive services and introduce a rount trip time scheme for propagation delay compensation to show that it satisfies the requirement. It was shown that the simulation results considering hardware impairments achieved an ATS accuracy of 0.5 μs or less even in a poor propagation environment.

Keywords—Absolute Time Synchronization, Round-Trip Time, Wireless Time-Sensitive Service

I. INTRODUCTION

The wireless time-sensitive service has been gradually introduced in various fields such as factory automation, collaborative robots, and collaborative drones, and is expected to be spotlighted as a key application field in 6G. It requires wire-level reliability and ultra-low synchronization error among devices to be guaranteed. ITU-TSG13, an international standardization organization, presented a high-precision service as a service of 6G, and began research on new network protocols and structures of 6G through the NET2030 Focus Group [1]. Examples of high-precision services include collaborative driving and flight, and factory automation using collaborative robots. Among them, factory automation services are becoming increasingly wireless for easy to move and flexible operation. Accordingly, high-precise absolute time synchronization (ATS) on radio is required for sequential and isochronous operation at the wired level, where ATS stands for the synchronization of devices' timekeeping regardless of their locations. At this point, the allowable ATS error between devices is ±0.5 μs within a cycle time that includes message exchange procedures consisting of base station (BS) command, device action, and device response [2],[3]. ATS errors can damage production lines and cause work safety problems. However, considering the existing 4G long-term evolution (LTE) and 5G new radio (NR) standards, it is difficult to meet the ATS requirements for wireless time-sensitive service. In particular, in high-frequency bands such as 28 GHz, phase noise caused by hardware (HW) impairment has a significant impact, making it more difficult to meet the requirements. Therefore, it is important to ensure that the ATS requirements is consistent with channel changes in the wireless environment under the HW impairment.

In this paper, we propose an examplary frame structure suitable for meeting these ATS requirements and analyze the performance by applying the round-trip time (RTT) method for propagation delay compensation in the frame structure. Section II describes frame structure for wireless time-sensitive service, and Section III introduces RTT procedure description. In Section IV, we evaluate the ATS accuracies under various HW impairments and channel conditions, followed by conclusion in Section V.

II. FRAME STRUCTURE FOR WIRELESS TIME-SENSITIVE SERVICE

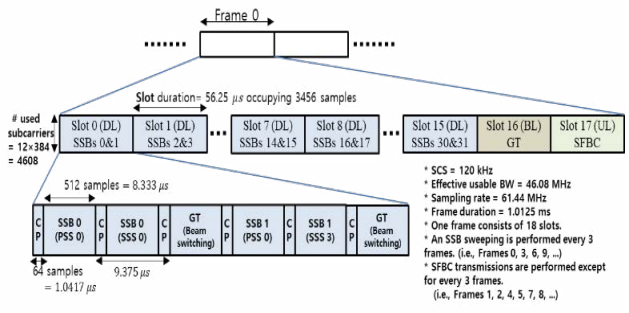

Fig. 1. The SSB sweeping frame structure for wireless time-sensitive service

Fig. 1 shows the proposed synchronization signal block (SSB) sweeping frame structure used in the initial state. The SSB sweeping frame consists of 16 downlink (DL) slots for SSB sweeping, one guard time (GT) slot and one uplink (UL) slot in total, with a frame length of 1.0125 ms. The SSB sweeping frame is transmitted once every three frames (i.e., Frames 0, 3, 6, 9, ...). One DL slot consists of 6 orthogonal frequency-division multiplexing (OFDM) symbols, each OFDM symbol with a length of 9.375 μs consists of one 64-sample cyclic prefix (CP) and one 512-sample effective OFDM symbol. Each slot length is 56.25 μs. One DL slot beam sweeps two SSBs, and one SSB consists of 3 OFDM symbols, such as beamformed primary synchronizaiotn singal (PSS), secondary synchronization signal (SSS), and GT for beam switching. Here, different SSBs are composed of different beams, and the PSS for each SSB is the same regardless of the SSB ID, but the SSS is mapped to the SSB ID and is different from each other. That is, the PCI of the SSS specified in 5G NR is mapped to the SSB ID one-to-one. For example, SSS 0 in SSB 0 is a frequency domain synchronization signal referring to PCI 0, and SSS 3 in SSB 1 is a frequency domain

synchronization signal referring to PCI 3. Specifically, there are 16 DL slots, so 32 SSBs can be swept. In Fig. 1, slot 16 is a GT slot that switches from DL to UL, takes up time corresponding to 6 OFDM symbols as described above, and the last UL slot 17 is a UL slot for reporting control information obtained from DL to UL.

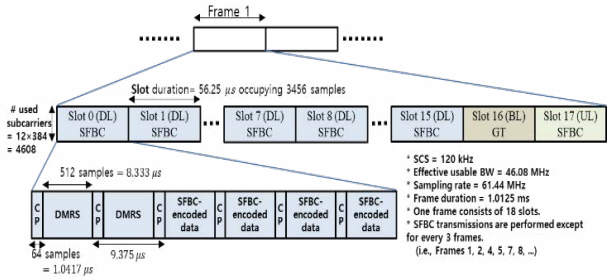

Fig. 2. The frame structure for the SFBC data transmission

Fig. 2 shows an examplary space frequency block coding (SFBC) frame structure for data transmission. The SFBC transmission frame consists of 16 DL slots for SFBC transmission, one GT slot, and one UL slot, with a frame length of 1.0125 ms as shown in Fig. 2. SFBC transmission frames are transmitted twice every three frames (i.e., Frames 1, 2, 4, 5, 7, 8, ...), one DL slot consists of 6 OFDM symbols, each OFDM symbol with a length of 9.375 μs consists of one 64-sample CP and one 512-sample effective OFDM symbol, and the slot length is 56.25 μs. One DL slot consists of two demodulation reference signal (DMRS) symbols for channel state information (CSI) estimation and refined downlink synchronization and four SFBC-encoded data symbols for diversity gains. In Fig. 2, there are 16 DL slots, 232 bits per slot, and 3,712 bits are transmitted per SFBC transmission frame, and these SFBC transmission frames are transmitted twice every three frames. Thus, the total number of SFBC transmitted bits in three frames is 7,424 bits, which is spread to a transmission rate of 2.44 Mbps (=7,424/(1.0125*3)). Note that 720p high definition (HD) video playback is possible at this transmission rate. In the Fig. 2, slot 16 is a slot that switches from DL to UL, takes up time corresponding to 6 OFDM symbols as described above, and the last UL slot 17 is a UL slot for reporting control information obtained from DL to UL, DMRS and sounding reference signal (SRS) for CSI channel estimation and uplink synchronization, respectively, and SFBC encoded and transmitted to BS for diversity gains.

III. RTT Procedure Description

In 3GPP, both user equipment (UE)-side and BS-side propagation delay compensation (PDC) schemes are specified. This paper deals with the BS-side PDC scheme. Fig. 3 shows the procedure and error components for BS-side RTT. In the beginning, the BS wants to transmit signal (i.e., a PSS signal) at $\boldsymbol{t_1}$ to the UE. However, the DL signal is actually transmitted (Tx) at $\boldsymbol{t_{1,a}}$ due to DL Tx timing error ($e_{BS,\,DL,\,TX}$). The DL signal arrives to the UE at $\boldsymbol{t_{2,a}}$, where $\boldsymbol{t_{2,a}} - \boldsymbol{t_{1,a}}$ is the DL propagation delay. The UE detects that the DL signal is received (Rx) at $\boldsymbol{t_2}$ due to DL Rx timing error ($e_{UE,DL,RX}$). Then, the UE wants to transmit signal at $\boldsymbol{t_3}$, but the UL signal (identical to the DL signal) is actually transmitted at $\boldsymbol{t_{3,a}}$ due to UL Tx timing error ($e_{UE,\,UL,\,TX}$). The UL signal arrives to the BS at $\boldsymbol{t_{4,a}}$, where $\boldsymbol{t_{4,a}} - \boldsymbol{t_{3,a}}$ is the UL propagation delay. BS detects the signal at $\boldsymbol{t_4}$ due to UL Rx timing error ($e_{BS,\,UL,\,RX}$) [4].

Theoretical RTT is as follows :

$$RTT_{theoretical} = t_{4,\,a} - t_{1,\,a} - (t_{3,\,a} - t_{2,\,a}).$$

Actual RTT is as follows:

$$\begin{aligned} RTT_{actual} &= t_4 - t_1 - (t_3 - t_2) \\ &= t_{4,\,a} + e_4 - t_{1,\,a} + e_1 + t_{2,\,a} + e_2 - t_{3,\,a} + e_3 + e_5 \\ &= RTT_{theoretical} + e_1 + e_2 + e_3 + e_4 + e_5. \end{aligned}$$

Assuming total ATS error $e_{tot,NW-side\,RTT}$ is equal to total error($e_{tot,\,UE-side\,RTT}$) due to channel reciprocity,

$$e_{tot,\,NW-side\,RTT} (= e_{tot,\,UE-side\,RTT}) = \frac{e_{BS,\,DL,\,TX} + e_{UE,DL,RX} + e_{UE,\,UL,\,TX} + e_{indication} + e_{BS,\,UL,\,RX}}{2},$$

where $e_{indication}$ is to reflect the error due to report granularity of Rx-Tx time difference.

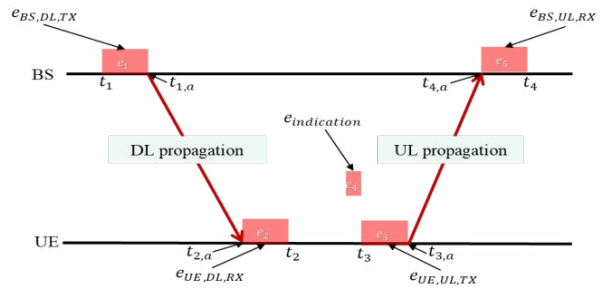

Fig. 3. Procedure and the total error for BS-side RTT based PDC

IV. Performance Evaluation

The performances of the RTT based PDC schemes are evaluated with the parameter settings listed in Table I.

TABLE I. Evaluation Parameters

Parameter	Value
SCS η [kHz]	120
Carrier frequency [GHz]	28
IFFT size N (DL)	512
Channel model	TDL-A & 3 km/h
RMS delay spread [ns]	66 [TR38.901, UMi Street-canyon normal delay prifile]
Cell deployment	1 NodeB, 1 UE
Residual CFO [ppm]	0.15
Phase noise β [5]	0.1/0.4
Time drift	NA
$e_{BS,\,DL,\,TX}$ [ns]	Uniformly distributed within [-48, 48]
$e_{UE,\,UL,\,TX}$ [ns]	Uniformly distributed within [-80, 80]
$e_{indication}$ [ns]	Uniformly distributed within [-8, 8]

In these performance evaluations, the two performance metrics are used as the following: 1) detection error ratio (DER); and 2) root mean square error (RMSE) of sample time offset (STO). The DER, one performance metric, defines that a successful detection is declared if the detected

STO is within ±0.25 μs[1]. Otherwise, an error is declared. This DER is considered the outage probability that the absolute value of the detected STO exceeds the required absolute value of STO, and is therefore the most important performance measurement in wireless time-sensitive service such as factory automation that requires specific timing accuracy and high reliability. In terms of DER, this paper compares NR PSS with the Beyond-Radio (BR) PSS designed by K. Chang, et al. [5] to be resistant to phase noise. Fig . 4 shows the DER performance as a function of SNR for the PSS detection when the channel models are TDL-A and TDL-D, where the values of phase noise (β) are 0.1 and 0.4 to be under harsh phase noises. It can be seen that BR shows better DER performance under all conditions compared to NR. Specifically, based on DER 10^{-3}, an SNR gain of approximately 0.5 dB is acheived when $\beta = 0.1$, On the other hand, when $\beta = 0.4$, the NR has flows between DER 10^{-2} and DER 10^{-3}, but BR shows stable DER performance in both TDL-A and TDL-D channels.

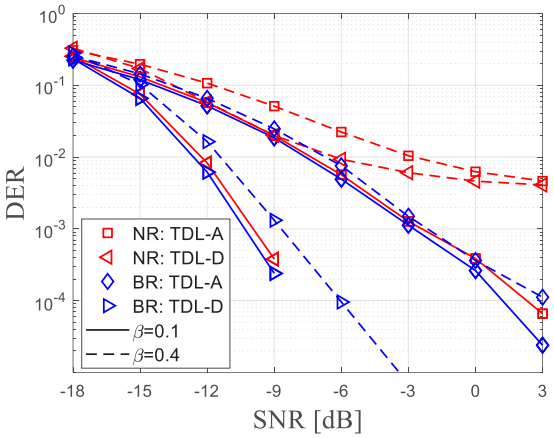

Fig. 4. DER versus SNR per Rx antenna

The RMSE, another performance metric, defines taking root in the mean of the square of the difference between the estimated STO [μs] $\hat{\epsilon}_{sto}$ and the required STO [μs] ϵ_{sto} as

$$RMSE_{sto} = \sqrt{\sum_{i=0}^{Q-1}(\epsilon_{sto} - \hat{\epsilon}_{sto})^2 / Q},$$

where Q is the number of simulation drops. Fig. 5 shows the RMSE performance as a function of SNR when the channel models are TDL-A and TDL-D, where the values of phase noise (β) are 0.1 and 0.4 to be under harsh phase noises as in Fig. 4. In Fig. 5, it can be seen that the SNR satisfying the STO requirement of 0.25 μs is -12 dB in BR (TDL-D, $\beta = 0.4$), which is 3 dB higher than BR. In addition, Fig. 5 shows that while the difference between the two is relatively small when $\beta = 0.1$, the performance gap is larger when $\beta = 0.4$.

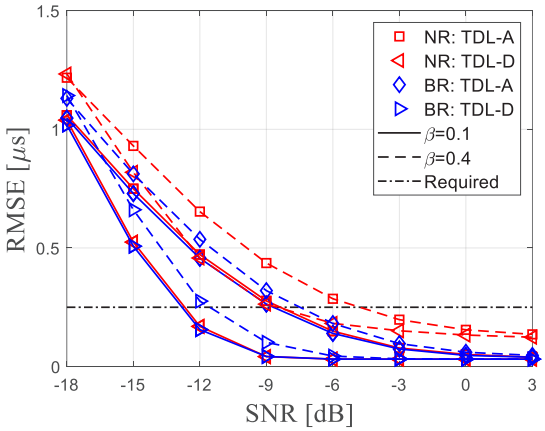

Fig. 5. RMSE versus SNR per Rx antenna

V. Conclusion

This paper has presented a new frame structure to meet the stringent ATS accuracy requirement of ±0.25 μs for the wireless time-senitive services, which are expected to play a pivotal role in the upcoming 6G era. On top of the structure, the RTT procedure specified in 3GPP Rel-17 has been executed. During this process, the NR PSS and the BR PSS proposed in our previous work have been employed as timing reference signals for performance comparison. Performance evaluations based on DER and RMSE metrics have demonstrated that employing the BR PSS leads to achieving the targeted ATS accuracy of ±0.25 μs at lower SNR levels, in contrast to using the NR PSS.

Acknowledgment

This work was supported by Institute of Information & communications Technology Planning & Evaluation (IITP) grant funded by the Korea government(MSIT) (No.2018-0-00218, Speciality Laboratory for Wireless Backhaul Communications based on Very High Frequency)

References

[1] "Towards a New Internet for the Year 2030 and Beyond," ITU IMT2020/5G Workshop, July 2018.

[2] TR 22.804; "5G for Connected Industries and Automation", 5G ACIA White Paper, April 2018.

[3] 3GPP TR 22.804, "Technical specification group services and system aspects; Study on communication for automation in vertical domains," Dec. 2017.

[4] Qualcomm Incorporated, "Enhancements for support of time synchronization for enhanced URLLC/IIoT" R1-2101463, 3GPP TSG-RAN WG1 Meeting #104-e-Meeting, Jan. 25th – Feb. 5th, 2021.

[5] K. Chang, W. Cho, B.-J. Kwak, and Y.-J. Ko, "Synchronization under hardware impairments in over-6-GHz wireless industrial IoT Systems," *IEEE IoT-J*, vol. 10, no. 7, pp. 6082-6099, April 1, 2023.

[1] It is expected that the 6G will require a higher level of timing synchronization accuracy than 1 μs mentioned in 5G applications, so 0.5 μs is set to decision bound.